Developmental Biology 437 (2018) 131–139

Contents lists available at ScienceDirect

Developmental Biology

journal homepage: www.elsevier.com/locate/developmentalbiology

Dispersing movement of tangential neuronal migration in superficial layers of the developing chick optic tectum

Yuji Watanabe*, Chie Sakuma, Hiroyuki Yaginuma

Department of Neuroanatomy and Embryology, School of Medicine, Fukushima Medical University, Fukushima 960-1295, Japan

ARTICLE INFO

Keywords:
Cell migration
Optic tectum
Time-lapse
Chick

ABSTRACT

During embryonic brain development, groups of particular neuronal cells migrate tangentially to participate in the formation of a laminated structure. Two distinct types of tangential migration in the middle and superficial layers have been reported in the development of the avian optic tectum. Here we show the dynamics of tangential cell movement in superficial layers of developing chick optic tectum. Confocal time-lapse microscopy in organotypic slice cultures and flat-mount cultures revealed that vigorous cell migration continued during E6.5–E13.5, where horizontally elongated superficial cells spread out tangentially. Motile cells exhibited exploratory behavior in reforming the branched leading processes to determine their pathway, and intersected with each other for dispersion. At the tectal peripheral border, the cells retraced or turned around to avoid protruding over the border. The tangentially migrating cells were eventually distributed in the outer *stratum griseum et fibrosum superficiale* and differentiated into neurons of various morphologies. These results revealed the cellular dynamics for widespread neuronal distribution in the superficial layers of the developing optic tectum, which underline a mode of novel tangential neuronal migration in the developing brain.

1. Introduction

The optic tectum in non-mammalian vertebrates and the superior colliculus in mammals have multi-layered structures. The superficial layers receive visual inputs through retinal ganglion cell axons, and the deeper layers perform integration of multiple sensory modalities and output function (King, 2004; Butler and Hodos, 2005). The avian optic tectum is composed of 15 layers subdivided by distinct neuronal cell types (Ramón y Cajal, 1911; LaVail and Cowan, 1971a; Senut and Alvarado-Mallart, 1986). Tectal layers are formed primarily by radial migration of post-mitotic neuronal cells from the ventricular layer to their destination, depending on their time of birth (LaVail and Cowan, 1971b; Gray et al., 1988; Gray and Sanes, 1991; Sugiyama and Nakamura, 2003).

During brain development, groups of particular neuronal cells migrate tangentially. It has been extensively studied in the mammalian cerebral cortex that cells originating from ganglionic eminences migrate tangentially towards the cortex in order to give rise to GABAergic interneurons (Anderson et al., 1997; Parnavelas, 2000; Corbin et al., 2001; Lambert de Rouvroit and Goffinet, 2001; Marín and Rubenstein, 2001; Nadarajah and Parnavelas, 2002). Cajal-Retzius cells derived from the discrete regions of the pallium migrate superficially in tangential directions to colonize the entire cortex (Bielle et al., 2005; Meyer et al., 2002; Takiguchi-Hayashi et al., 2004). Additionally, in the developing hindbrain, precerebellar neurons generated in the rhombic lip migrate circumferentially around the medulla to form the inferior olive, the lateral reticular and the external cuneate nuclei (Harkmark, 1954; Altman and Bayer, 1987a, 1987b; Bourrat and Sotelo, 1988, 1990; Tan and Le Douarin, 1991; Ambrosiani et al., 1996; Ono and Kawamura, 1989; Kawauchi et al., 2006).

In the avian optic tectum, two streams of tangential migrations in the middle and superficial layers have been reported using Golgi staining, retrovirus-mediated cell labeling, and quail-chick chimeric transplants (Domesick and Morest, 1977; Puelles and Bendala, 1978; Gray and Sanes, 1991; Martínez et al., 1992). Recently, the movement of the tangentially migrating cells in the middle layers (prospectively in the deep layers) has been visualized by time-lapse recording of fluorescent-labeled cells in tectal tissue culture (Watanabe et al., 2014; Watanabe and Yaginuma, 2015). During E6–E8, tangential migrants with a bipolar cell shape move in an axophilic way, clinging to the fasciculus of tectal efferent axons in the prospective stratum album centrale (SAC). After E8, they translocate toward the upper layers to differentiate into multipolar neurons in the stratum griseum centrale (SGC) (Domesick and Morest, 1977; Puelles and Bendala, 1978; Watanabe et al., 2014). On the other hand, the mode of tangential migration in the superficial layers remains elusive; this

* Corresponding author.
E-mail address: yuji-w@fmu.ac.jp (Y. Watanabe).

https://doi.org/10.1016/j.ydbio.2018.03.010
Received 17 January 2018; Received in revised form 10 March 2018; Accepted 12 March 2018
Available online 14 March 2018
0012-1606/

includes cell behavior, range, duration, direction of migration, and cell fate.

In the current study, we show the dynamics of tangential cell migration in superficial layers of the developing chick optic tectum. Time-lapse analysis revealed dispersing movement of individual cells with branched leading processes, which were reforming to find out the pathway to proceed for spreading. Motile cells exhibited exploratory behavior to avoid protruding over the tectal peripheral border. These results reveal cellular dynamics for the widespread distribution of neurons in the superficial layers in the developing optic tectum, which underline a mode of novel tangential neuronal migration in the developing brain.

2. Results

2.1. Tangential migration in superficial layers in tectal slice culture

In our previous study, we noticed horizontally elongating cells in sections of the superficial layers of the chick optic tectum during E7.5–E10.5, which were supposed to migrate tangentially (Watanabe et al., 2014). To outline the tangential movement in the layered structure, we first monitored tangential migration of fluorescently-labeled cells in a tectal slice culture. Using Tol2-mediated gene transfer for stable transgene expression (Sato et al., 2007), the expression vectors encoding EGFP and mCherry with nuclear localizing signal (mCherry-Nuc) were co-electroporated into E1.5 mesencephalon for overall labeling of the neuroepithelial cells in the prospective tectal wall. Slice culture of the labeled tectal tissue was conducted at E7.5 to monitor cell behavior under confocal time-lapse microscopy.

Video 1 shows time-lapse images taken every 10 min over a period of 20 h (among N = 6 specimens visualized). Horizontal cell movement was remarkable in the upper layers, especially in the marginal cell sparse zone above prospective layer VI (layer nomenclature after LaVail and Cowan, 1971a). There were few cells that left from the superficial tangential stream, indicating that the passable layers for tangential migration were confined. Individual migrating cells had a long and motile leading process extending toward the proceeding direction, and exhibited saltatory movements intermitted by short periods of slow movement. Nuclear movement (mCherry-Nuc) indicated that overall cell speed was not decreased over time, and was sustained throughout the whole observation period. Migration occurred all over the tectal surface in the cultured slice. Video 2 follows the movement of an arrow select cells from Video 1 in higher magnification. While some cells procceded unidirectionally along the dorso-ventral axis (red or blue arrow directed dorsoventrally; light blue arrow directed ventrodorsally), another cell seemed to wander by turning back several times (yellow arrow). These observations suggest that the tangential migration of the labeled cells was active in the superficial layers, where the cells might be moving horizontally in non-linear manner.

Supplementary material related to this article can be found online at http://dx.doi.org/10.1016/j.ydbio.2018.03.010.

2.2. Tangentially migrating cells spread in superficial layers

While the slice culture system recapitulated the tangential movement specific to the superficial layers, it did not reveal cell behavior or the directionality of migration on the horizontal plane. Therefore, we set up focal fluorescent labeling on the tangential migrants and performed a flat-mount culture to observe cell movement on the horizontal plane in the superficial layers.

In a previous study, we reported that electroporation at E4.5 enabled labeling of neuroepithelial cells in the ventricular layer, which migrated radially and eventually turned to join both the middle and superficial streams as tangentially migrating cells (Watanabe et al., 2014). After adjusting the timing of electroporation, we found that superficial migrating cells were predominantly labeled when the electroporation was performed at E5.5 (Fig. 1). Two days after focal labeling by electroporation, dorsal and ventral streams of superficial migrants had been emigrating from the radially arranged columns of GFP-positive cells (Fig. 1A; open and closed arrow, respectively; N = 3). In a case when a large area was labeled by electroporation, the superficial migrants were scattered broadly on the tectal surface at E10.5 (Fig. 1B–F; N = 3), suggesting that the migrating cells spread ubiquitously throughout the superficial layers.

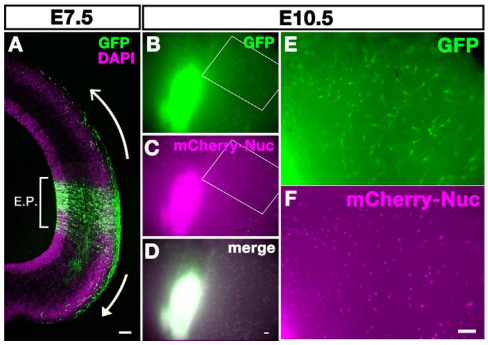

Fig. 1. Labeling of tangentially migrating cells, which spread over the tectal surface. Electroporation was performed at E5.5 into a portion of the tectal wall to transfect the pCAGGS vectors expressing EGFP and mCherry-Nuc. (A) The dorsal and ventral stream of superficial migrants emigrated from the radially arranged columns of GFP-positive cells at E7.5 (open and closed arrow, respectively). (B–D) When a large area was labeled by electroporation, the superficial migrants from the labeled columns were scattered broadly on the tectal surface at E10.5. (E, F) A higher magnification view of the area enclosed by a white box (B, C). Scale bars; (A) (B–D) (E, F) 100 μm.

2.3. Dispersing movement of superficial migration

It is noteworthy that the labeled cells stayed superficial during the thickening of the tectal layers, because these layers develop extensively under the tangential stream. We speculated that this superficial disposition of the migrating cells should facilitate our observation on the superficial migration from the pial side within the focal length. Therefore, we applied a flat-mount culture of labeled tectal tissue on the culture insert and traced the cell movement on the horizontal plane from the pial side. The expression vectors encoding EGFP and mCherry-Nuc were focally electroporated at E5.5. Tectal tissue was cut at E7.0 and laid pia-side down on the culture insert in a glass-bottom dish to monitor cell behavior by confocal time-lapse imaging under an inverted microscope.

Overall movement of tangential migration was captured as time-lapse images taken every 10 min over a period of three days from E7.0 (E7-E9, Video 3; N = 4). At the onset of culture, fluorescent labeling was focused on an electroporated area (approximately 300 × 400 μm) as revealed in the nuclear distribution of mCherry-Nuc (Video 3, right panel).

At the initial phase (0–24 h), the labeled emigrating cells left from the labeled area, and proceeded preferentially in dorsal and ventral directions. After the initial phase (24–48 h), the following cells left the labeled area and spread in various directions. In the latter phase (48–72 h), the migrating cells had broadly scattered to the surrounding region of the spot. The migration was multi-directional but not simple linear radial dispersion because the migrating cells occasionally changed direction. Each cell had a long leading process, which stretched over 100 μm at the maximum and changed length during migration. The leading process sometimes sprouted a new branch, which might have triggered the steering of the migration direction. The cells intermittently paused during migration before directional change, and subsequently migrated steadily again. As a result, the migration was neither radial nor erratic, but multi-directional, in that the migrating cells from the labeled area were dispersing out in various directions.

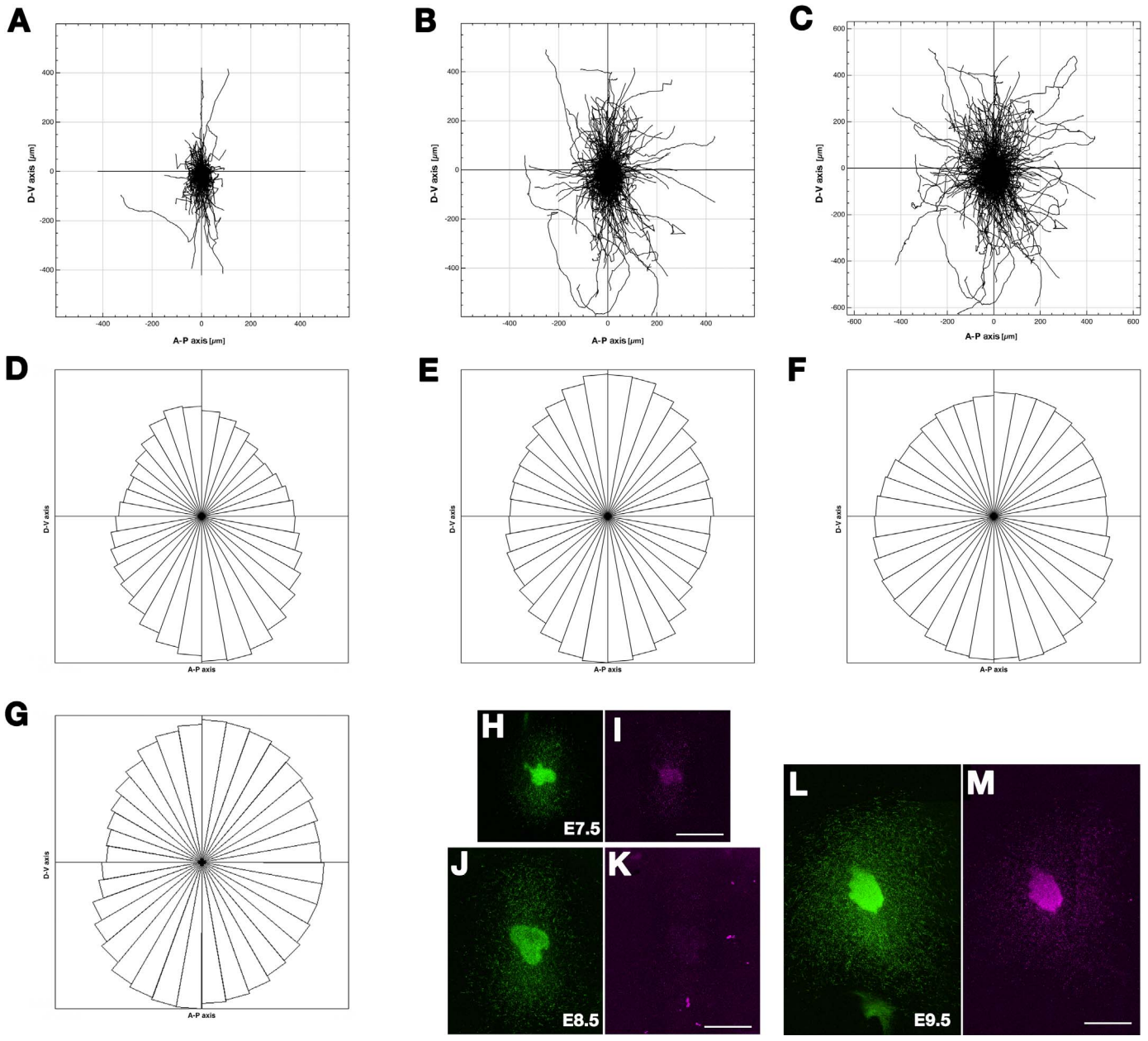

Fig. 2. Trajectories of tangential migration. (A-C) The cumulative migration trajectories of Video 4 were plotted on the graph in which the migration start points were assembled at the origin of the coordinates. Scale on x and y axes: 50 μm. (A) 0–24 h, (B) 0–48 h, (C) 0–72 h. (D-F) Rose diagrams showing the distribution of migration angles of Video 4 (D) and two other experiments of the same condition (E, F) over three days. (G) A rose diagram showing the distribution of migration angles of Video 6 over two days. (H-M) Dispersion of the migrating cells at E7.5 (H, I), E8.5 (J, K) and E9.5 (L, M) showing the localization of GFP-labeled cells (H, J, L) and mCherry-labeled nuclei (I, K, M). Dorsal to the top and anterior to the right. Scale bars; (H, I) (J, K) (L, M) 1 mm.

The directionality of migration was analyzed by following the trajectories of the nuclear movement. With regard to the nuclear movement of mCherry-Nuc (Video 3, right panel), a definite signal from the cell nuclei was traced using automatic particle tracking (Video 4). The cumulative migration trajectories were plotted on the graph in which the migration starting points were assembled at the origin of the coordinates (Fig. 2A-C). In one day (0–24 h), the trajectories preferentially directed to the dorsal and ventral directions (Fig. 2A). In two days (0–48 h), anterior or posterior projections emerged and added to the bilateral dorsal and ventral projections (Fig. 2B). Over three days (0–72 h), total projections became omnidirectional (Fig. 2C). Finally, the directionality of the nuclear migration in Video 4 and the other two experiments of the same condition over the three days were analyzed (Fig. 2D–F; N = 3). Rose diagrams showing the distribution of the migration angles indicated that the angles were distributed all directions while deflected to elliptic shape along the dorso-ventral directions.

The shift of cell trajectories from dorso-ventral in early phase to ominidirectional in later phase was confirmed by starting the culture from the later day after electroporation. After two more incubation days in ovo, tangential movement was examined in flat-mount culture from E9.0 (E9-E10, Video 5; N = 3), which corresponded to the later phase of the culture from E7.0 (Video 3 and 4). The trajectories of migration was no longer preferential in dorsal and ventral directions, but ominidirectional throughout the culture period, which was also revealed by the particle tracking (Video 6) and the rose diagram of the migration angles (Fig. 2G).

Supplementary material related to this article can be found online at http://dx.doi.org/10.1016/j.ydbio.2018.03.010.

Dispersion of the migrating cells was further examined by observing

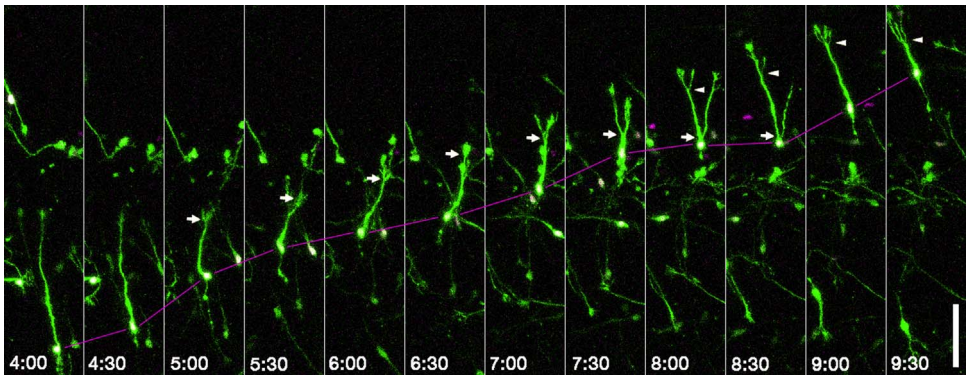

Fig. 3. Remodeling of the leading process during migration in time-lapse sequence. Typical cycles of a branching process during migration were extracted from Video 7 in a time-lapse sequence. The elapsed time is shared with Video 7 and 8. The magenta line represents the displacement of the nucleus. An arrow and an arrowhead denote the first and second branching points of the leading process, respectively. The same images are included in Video 8. Scale bar; 100 μm.

the horizontal localization of the spreading cells in a wide range. After the electroporation at E5.5, the labeled tectum was excised at E7.5, E8.5, E9.5, and flat-mounted (Fig. 2H-M). At E7.5, the emigrating cells were densely localized at dorsal and ventral vicinity of the labeled area (Fig. 2H, I; N = 3). At E8.5, the cells had extensively spread into the dorsal and ventral directions and also moderately dispersed in the anterior and posterior directions, presumably owing to the migration shift from dorso-ventral to ominidirectional projection (Fig. 2J, K; N = 3). At E9.5, the cells had distributed over the broader regions in elliptic shape along the dorso-ventral directions (Fig. 2L, M; N = 2). These results indicate that the tangentially migrating cells disperse broadly along the dorso-ventral axis.

2.4. Remodeling of the leading process drives directional change of the migration

The behavior of the individual cells was monitored in higher magnification (Video 7; N = 5). The migrating cells frequently repeated the remodeling of the leading process by branching. Typical cycles of a branching process of a cell denoted by the yellow arrow in Video 7 were revealed in a time-lapse sequence (Video 8; Fig. 3). A migrating cell of a bipolar shape proceeded smoothly and linearly (t = 4:00–5:00; the magenta line denotes the displacement of the nucleus in Fig. 3). The motile leading process occasionally branched from the growth cones at the distal end of the process (t = 5:00; an arrow indicates the branching point), followed by forward movement of the soma and nucleus (t = 5:00–7:00). Subsequently, the soma and nucleus approached the branching point to bifurcate the leading process (t = 7:00–8:00). One of the branches further elongated to lead the pathway choice, and the soma and nucleus followed the selected branch, while the other branch retracted to join as a trailing process (t = 8:00–9:00). The selected leading process sprouted a new branch (t = 8:00–9:30; the arrowhead indicates the new branching point) and the soma and nucleus again approached the new branching point (t = 8:30–9:30). While the soma with the nucleus displaced rapidly when the cell was bipolar (t = 4:30–5:00), including the phase just after the pathway choice (t = 8:30–9:30), it displaced slowly or was stationary during the pathway decision process (t = 7:30–8:30). These observations suggest that the remodeling of the leading process drives directional change to steer the trajectory of migration.

Supplementary material related to this article can be found online at http://dx.doi.org/10.1016/j.ydbio.2018.03.010.

2.5. Intersection of the migrating cells from different origins

The horizontal dispersion of the tangentially migrating cells in the superficial layers observed so far was reminiscent of the migration of Cajal-Retzius (CR) cells in the surface of the developing mammalian cerebral cortex (Bielle et al., 2005; Meyer et al., 2002; Takiguchi-Hayashi et al., 2004). In the case of CR cells, cell-cell repulsive interactions were suggested to restrict the relative distribution of CR cells from different origins in a contact-dependent manner (Villar-

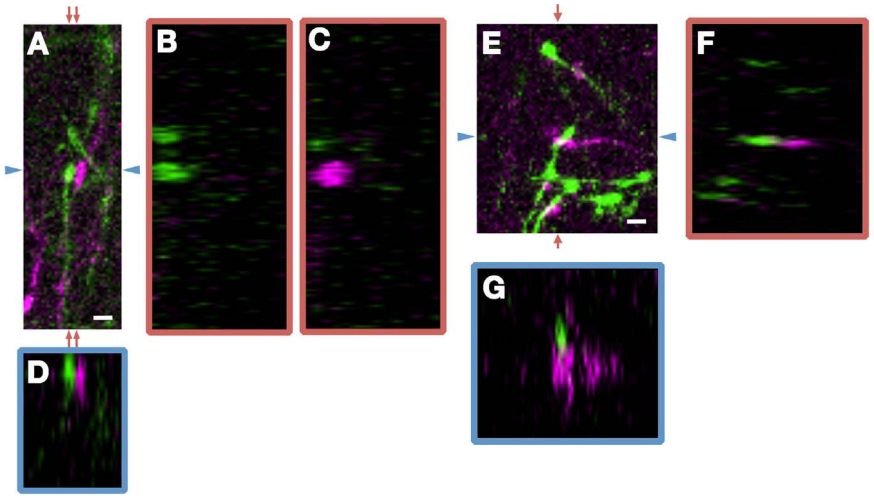

Fig. 4. Intersection of the migrating cells from different origins. The spatial relationship between the migrating cells from different origins was examined when they were encountered in close proximity. Images of (A) and (E) were extracted from the lower panel of Video 9. The images of the confocal plane are indicated by red arrows or blue arrowheads in (A) and (E) are shown in red (B, C, F) or in blue (D, G) frames. GFP in green, mCherry in magenta. (A–D) When two migrating cells were passing each other in opposite directions, they proceeded side by side in the same horizontal plane. (E–G) When the cells were crossing, they intersected each other on different horizontal planes. Scale bars; (A–D) (E–F) 10 μm.

Cerviño et al., 2013). We then questioned whether a similar cellular response could take place when tectal superficial migrants of different origins were encountered.

Two tectal regions more than 500 μm apart were labeled in the GFP and mCherry, and encounters of the labeled cells of different fluorescence in between the two regions were observed over two days (Video 9; N = 3). As in Video 3, both GFP- and mCherry-positive cells first preferred proceeding along the dorso-ventral axis, and shifted to omnidirectional displacement. After the two groups of cells were encountered each other (after t = 12:00), each group seemed to proceed regardless of the behavior of the other group; however, individual cells occasionally changed direction to proceed. The spatial relationship between the migrating cells that were crossing in close proximity to each other was examined (Fig. 4). In a case when the cells passed by toward opposite directions (Fig. 4A), they proceeded side by side (Fig. 4D) in the same horizontal plane (Fig. 4B, C). In another case when they were crossing (Fig. 4E), they intersected each other on different horizontal planes (Fig. 4F, G). These observations suggest that while mutual repulsion between groups of migrating cells from different origins was not prominent, the encountering cells mutually pass by or intersect to disperse into broader tectal superficial areas.

Supplementary material related to this article can be found online at http://dx.doi.org/10.1016/j.ydbio.2018.03.010.

2.6. Caged migration enclosed by tectal peripheral border

In the later stage of development, as the labeled tangential migrants dispersed broadly throughout the tectal surface (Fig. 1B-D), they were rarely detected outside of the tectal territory, including the tegmental region (data not shown). We then focused our interest on how transboundary migration is restricted at the tectal peripheral border. After labeling the ventral tectal area near the boundary between the tectum and the tegmentum, we concentrated on the migration of the ventrally approaching cells toward the boundary over two days (Video 10; N = 3). The ventrally migrating cells approached the boundary but changed direction before invading across the border. Individual cell

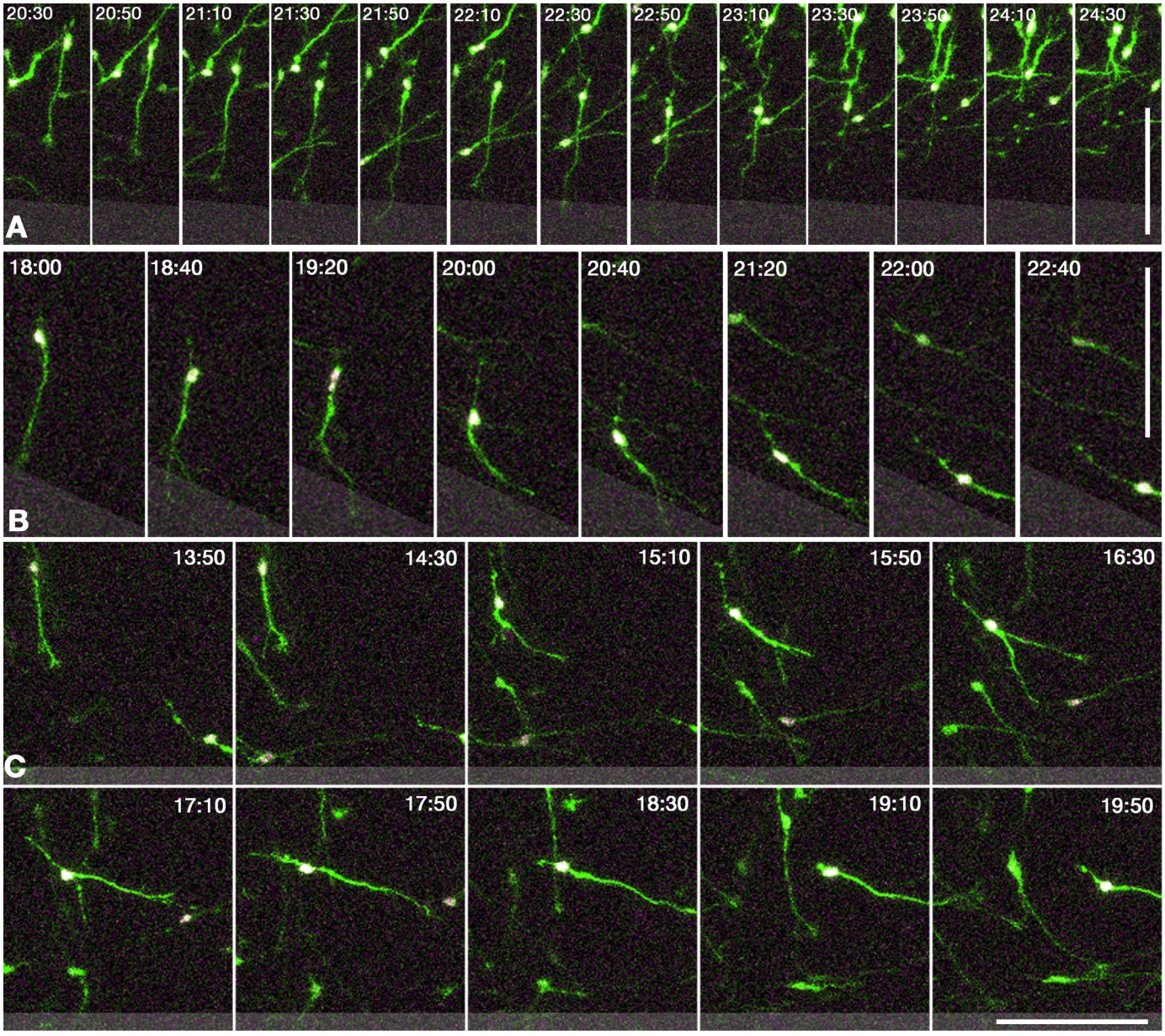

Fig. 5. Cell behavior at the tectal peripheral border. Cell behavior at the border of the optic tectum (upper black area) and the tegmentum (lower gray area) was extracted from the lower left panel of Video 10 in a time-lapse sequence. Note that the tegmental area is demarked by the anteriorly extending longitudinal axons in Video 10. Dorsal to the top and anterior to the right. (A) Retracing behavior, (B) Turning behavior, (C) Avoidance behavior at a distance of the border. Videos 11–13 share the same frames with A–C, respectively. Scale bar; 100 μm.

behavior was extracted (Fig. 5). Video 11 shows a cell perpendicularly approaching the boundary (Fig. 5A; tegmentum is denoted by lower gray area) while touching the border with its leading process (t = 21:50–22:30), then retracting the process (t = 22:50–23:30), switching back by transforming the trailing process to the leading process (t = 23:10–23:30) and returning toward the tectum (t = 23:30–24:30). In another case (Fig. 5B; Video 12), while touching the border (t = 18:00), the approaching cell repeatedly sprouted new branches to reform the leading process parallel to the border (t = 18:40–20:40) and proceeded along the border (t = 21:20–22:40). Another cell approaching the offset (Fig. 5C; Video 13) gradually changed direction by branching several times unless its leading process touched the border (t = 14:30–16:30), and selected a process parallel to the border (t = 17:10–19:50). No labeled cell was observed to have crossed the border (Video 10). The limit of migration at the boundary was strict because we did not detect any migrating cells that may have invaded into the tegmental area (among three independent experiments). Caged inside the tectal region, the dispersing cells made course corrections by remodeling their leading process to follow the border.

Supplementary material related to this article can be found online at http://dx.doi.org/10.1016/j.ydbio.2018.03.010.

2.7. Migration duration and cell destination

Observations on active migration in a flat-mount culture revealed that the tangential migration seemed to continue for at least several days. We wondered how long the tangentially migrating cells would keep moving. As observed in Video 3, a small number of cells had already started migration at E7.0. To elucidate the duration of migration, we first examined migration onset. After labeling the numbers of progenitor cells by electroporation at E1.5, we determined when the earliest cell migration had occurred in the flat mount culture. While no cells had moved when the culture was started at E6.0 (0% of 425 total fluorescent-labeled cells in the superficial layers), a small population of cells had begun tangential migration at E6.5 (4.0% of 353 cells), indicating that the migration starts after E6.5. We next surveyed the termination of migration by following the migrating cells in the culture. After labeling the migrating cells by electroporation at E5.5, we prepared a flat-mount culture each day to examine the daily shift of the proportion of the migrating cell number per labeled cell number, and the average velocity of migrating cells (Fig. 6). Whereas nearly all the labeled cells migrated at E7.5, the proportion of migrating cells declined to under 50% at E10.5, then reduced to less than 10% at E13.5; eventually, migration of all the labeled cells ceased at E14.5 (Fig. 6, blue bar). The average velocity of the migrating cells initially peaked at E7.5 (27 μm/h), and gradually declined over a period of seven days (Fig. 6, red line). Taken together, tangential migration occurs during E6.5–E13.5, with its peak number of migrating cells and velocity of migration at E7.5, both of which decay toward E14.5.

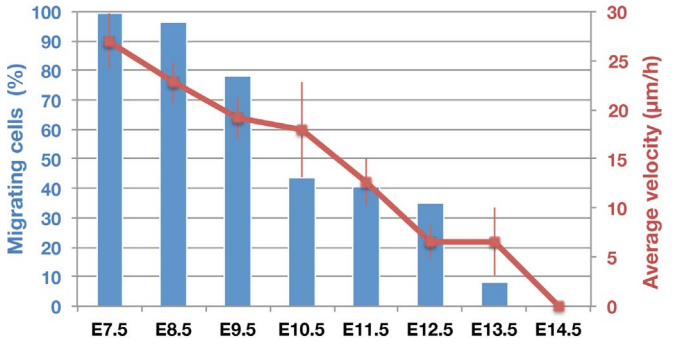

Fig. 6. Duration of the tangential migration. After labeling the migrating cells by electroporation at E5.5, a flat-mount culture was prepared each day to examine the daily shift of the proportion of migrating cell number per labeled cell number (blue bars; 169, 117, 156, 124, 151, 117, 73 and 43 labeled cells were examined for the video from E7.5, 8.5, 9.5, 10.5, 11.5, 12.5, 13.5 and E14.5, respectively). The average velocity of migrating cells (red lines; the velocity of 10 migrating cells was examined for each video) over 22 h. Both migrating cell number and velocity peaks occur at E7.5 and gradually decay towards E14.5.

We finally examined the fate of the tangentially migrating cells. At E18.5, two days before hatching, the labeled tangentially migrating cells were distributed within layers a–h in the upper SGFS (*stratum griseum et fibrosum superficiale*; Cowan et al., 1961), the outer layers of the optic tectum (Fig. 7A). These superfitial layers contained a variety of neuron types of different shapes and, notably, layers a and d included horizontally oriented cells with widely ramifying dendrites (Fig. 7A; LaVail and Cowan, 1971a). The layer distribution of the labeled cells after tangential migration indicated that 80% of the migrants were localized in layers a–d, immediately below the retinal fiber layer SO (*stratum opticum*) (Fig. 7B; 380 cells were examined). Immunostaining with neuronal markers revealed that 98% and 99% of the migrants differentiated into NeuN and HuC/D-positive neurons, respectively (Fig. 7C, D; each 190 cells were examined). These results indicate that the tangential migrants were eventually distributed in the upper SGFS to differentiate into neurons.

3. Discussion

Tangential migration in the superficial layers of the optic tectum was originally detected by the horizontal cell shape in Golgi staining (Puelles and Bendala, 1978), and later confirmed by retrovirus-mediated cell tracing and quail-chick chimeric transplants (Gray and Sanes, 1991; Martínez et al., 1992). In the present study, we visualized mass movement of the superficial tangential stream and the dynamics of individual cell behavior by long-term time-lapse recording. This is the first demonstration of the overall picture of superficial tangential migration during tectal layer formation.

The tangentially migrating cells observed in our experiments originated from radially migrating cells, which were labeled in the ventricular zone and climbed to the superficial layers to join the tangential stream (Fig. 1A). The preceding tangential stream during the first day of culture preferred to migrate in dorsal and ventral directions (Fig. 2A). Some guidance mechanism may govern this dorso-ventral preference for the initial migration. However, during subsequent days of culture, the tangential stream shifted to project omnidirectionally (Fig. 2B, C). These results suggest that after the initial phase, the migration cells might be released from the guidance along the dorso-ventral axis, and became dispersing autonomously. Through such transition of the migration direction, the tangentially migrating cells came to disperse broadly along the dorso-ventral axis (Fig. 2L, M). In addition, the tangential migrants emerged from different origins (Video 9). Omnidirectional migration from multiple origins may offer the basis of superficial migration covering the broad tectal surface (Fig. 1B-F).

Dispersing movement with a remodeling leading process is a typical behavioral characteristic of tectal superficial migration. The agile activity of the migrating cells can contribute to widespread neuronal dispersion and to spatial restriction within the range of the tectal region. The migrating cell senses the physical environment with the growth cone at the distal tip of its leading process. When the migrating cell encounters an obstacle, the cell can change direction and proceed by branching the leading process and choosing one of its branches to avoid the obstacle. Superficial layers after E7 are the traffic of tangentially migrating cells from different origins (Video 1), although only a limited number of cells from two separate domains were labeled in our flat-mount culture (Video 9). The migrating cells have many chances to contact with other tangentially migrating cells or with the grids of radially arranged cells, which may elicit branching behavior to avoid collision and repulsion and instead intersect and overcross as shown in Fig. 4 (Video 9). These exploratory cell movements can be attributed to even and ubiquitous distribution of tangential migrants.

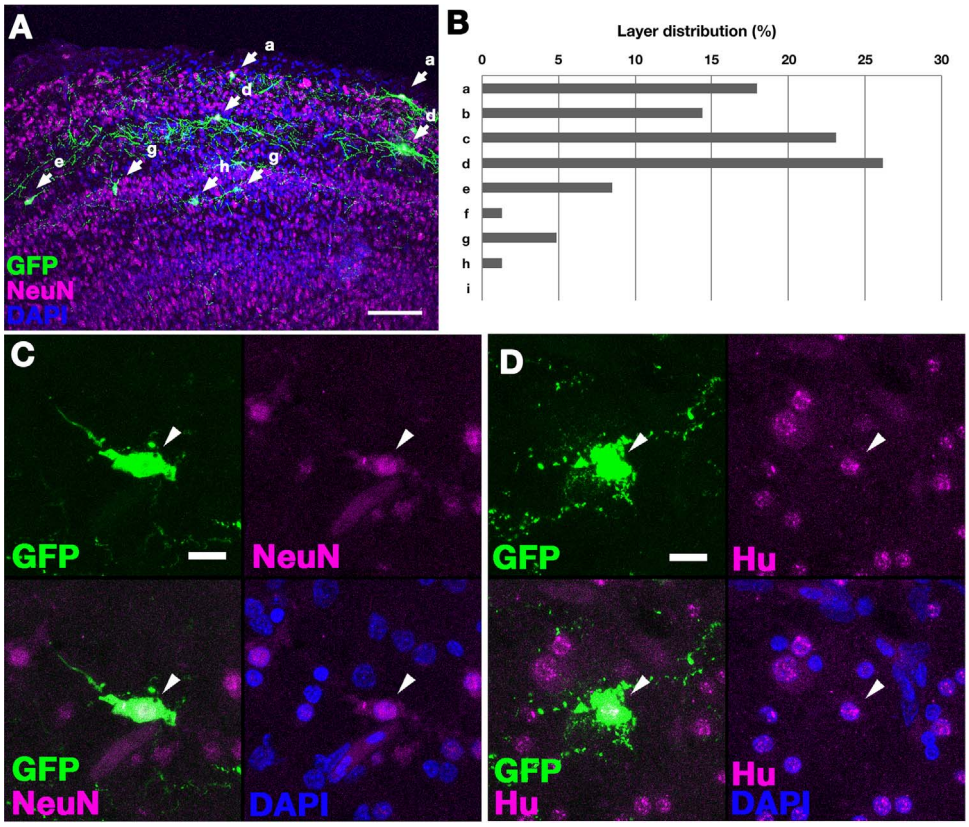

Fig. 7. Fate of the tangentially migrating cells. After labeling the migrating cells by electroporation at E5.5, the distribution of the labeled cells in the tectal layers (A, B) and the expression of neuronal markers (C, D) were examined at E18.5. (A) Superficial layers contained a variety of neuronal types with different shapes, which are denoted by arrows with layer position. (B) Labeled tangentially migrating cells distributed among layers a–h in the upper SGFS (*stratum griseum et fibrosum superficiale*), the outer layers of the optic tectum. (C, D) Immunostaining with the neuronal markers (NeuN, HuC/D) revealed that the tangential migrants eventually differentiated into neurons. Scale bars; (A) 100 μm, (C, D) 10 μm.

At the tectal peripheral border, the contact of the leading process with a physical barrier, such as the longitudinal axons running in the tegmentum, might trigger retracing or turning response of the migrating cells to prevent a transboundary movement (Fig. 5A, B; Video 11, 12). The turning response was also observed in the approaching cell before directly touching the border, indicating that short-range chemorepulsion may be involved for controlling caged tangential migration within the optic tectum (Fig. 5C; Video 13).

The superficial tangential migration in the optic tectum has similarities and dissimilarities with other tangential migration in the brain. The migrating cells had a variable leading process, which frequently branched to steer the direction. This typical movement is shared by other tangential neuronal migration, such as by cortical interneurons and Cajal-Retzius cells (Martini et al., 2009; Villar-Cerviño et al., 2013). Exploratory behavior with a branching process might be a common feature of dispersing migration into broad brain regions. Despite such dynamic similarities during migration, tectal tangential migration marks a distinctive character in its regional origin and fate. The origin of tangential migrants is not restricted to specific regions, and can basically arise from anywhere in the tectum after radial migration to join the tangential stream. In addition, following dispersing migration, the tangential migrants are interspersed broadly into multiple layers in the outer SGFS throughout the tectum, and eventually differentiate into neurons of various morphologies (Fig. 7A). Regional equivalency in origin and fate may be relevant to the organization of the optic tectum, which does not have functional localization. Since the optic tectum receives direct retinotectal projections over the whole tectal surface, each tectal region may need to build up a homogeneous local circuit. Ubiquitously-interspersed neurons after migration from different regional origins might be the prerequisite for such unbiased neuronal circuits over a global tectal hemisphere.

In conclusion, our analysis on superficial cell migration in the chick optic tectum provided new information on the mode of tangential neuronal migration in the developing brain. The optic tectum is comprised of multiple layers elaborated by radial and tangential migration, the latter of which includes two distinct types of tangential migration; in the middle and superficial layers (Watanabe and Yaginuma, 2015). In the middle layers, the bipolar cells migrate linearly in dorsal and ventral directions along the fasciculus of tectal efferent axons during E6–E8 (Gray and Sanes, 1991; Watanabe et al., 2014). In the superficial layers, the migrating cells disperse with branched leading processes to spread in various directions during E6.5–E13.5 (this study). Despite these differences, both tangential migrants are eventually distributed ubiquitously in the tectal hemisphere. After the onset of the two tangential migrations, retinal axons enter from antero-ventral tectum and spread across the whole tectal surface during E6.5–E12.5, which overlaps with 90° rotation of the tectal proper (Goldberg, 1974; McLoon, 1985). These events contribute to propagate the components of the tectal neuronal circuit in a horizontal plane. In future studies, we aim to elucidate how the superficial migrants gradually lose cell motility in the long term and shift to neuronal differentiation to be integrated into the tectal neuronal circuit.

4. Materials and methods

4.1. Electroporation

In ovo electroporation at E1.5 was performed as previously described (Funahashi et al., 1999; Watanabe and Nakamura, 2000). pCAGGS-T2TP (2 μg/μl), pT2K-CAGGS-EGFP (5 μg/μl) and pT2K-CAGGS-mCherryNuc (5 μg/μl) were injected into the mesencephalon

Table 1
Optical and scanning conditions of the confocal time-lapse imaging.

	objective	digital zoom	scanning size (dpi)	scanning interval along z-axis (μm)	number of scan along z-axis	scanning time (s)	interval (min)	total time (h)
Video 1	10 ×	1 ×	640 × 480	5	17	153	10	20
Video 3	10 ×	1 ×	1024 × 1024	10	10	191	10	72
Video 5	10 ×	1 ×	512 × 512	10	18	97	10	48
Video 7	20 ×	2 ×	512 × 512	5	14	75	5	24
Video 9	20 ×	1 ×	512 × 512	5	20	108	5	48
Video 10	20 ×	1 ×	800 × 600	5	18	246	10	48

between a pair of electrodes (LF610P4x1, Unique Medical Imada, Japan; Niwa et al., 1991, Sato et al., 2007, Watanabe et al., 2014). Four pulses of 25 V, 50 ms were charged in 1-second intervals by the electroporator (CUY21EDIT, BEX, Japan).

For in ovo electroporation at E5.5, a mixture of pCAGGS-EGFP (4 μg/μl) and pCAGGS-mCherryNuc (4 μg/μl) was injected into the aqueduct of the left optic tecta with a micropipette. The optic tectum was placed between a pair of forcep-type electrodes (LF646P3x3, Unique Medical Imada, Japan) perpendicular to the tectal wall. Dual pulses of a pre-pulse of 30 V, 1 ms with a 5-ms interval and four subsequent pulses of 6 V, 5 ms with a 10-ms interval were charged by the pulse generator (CUY21EX, BEX, Japan).

4.2. Slice culture

Slice culture of the optic tectum was performed based on the method previously described (Placzek and Dale, 1999; Omi et al., 2014). The optic tecta at E7.5 was embedded in 3% low melting temperature agarose dissolved in 1xHBSS. Slice coronal sections at 250 μm were cut along the dorso-ventral axis in cold HBSS with the vibratome. Tectal slices were transferred to a 35 mm glass-bottom dish (Matsunami), embedded in rat-tail collagen supplemented with 1xDMEM, and covered with the culture medium (60% Opti-MEM, 20% F12, 10% fetal bovine serum, 10% chick serum, 50 units/ml penicillin, 50 μg/ml streptomycin). The dish was then incubated on an inverted microscope (IX81, Olympus, Japan) in a humid chamber unit with a gas flow of 40% O_2 and 5% CO_2, and a controlled temperature of 38 °C. Images of GFP, mCherry, and differential interference contrast were captured through 10 × (UplanApo) objective by using a confocal laser scanning microscope (FV300, Olympus). For Video 1, the image of 640 × 480 dpi was captured every 5 μm along the z-axis to a depth of 80 μm. Z-stack images at every 10 min interval (153 s scanning time included) over a period of 20 h were collected to construct a time-lapse video (Table 1).

4.3. Flat-mount culture

Millicell CM-ORG cell culture insert (Millipore) was coated with 8 μg/ml Laminin and 80 μg/ml poly-L-Lysine. Tectal tissue electroporated at E5.5 was cut and laid pia-side down on a Millicell CM-ORG cell culture insert (Millipore), which was set on a 35 mm glass-bottom dish (Matsunami) filled with 1.1 ml of the culture medium described above. Fluorescent images of the flat-mount culture were captured through 10xUplanApo or 20xLCPlanFl objectives (Olympus). Optical and scanning conditions were listed in Table 1.

4.4. Data analysis

The time-lapse image was analyzed with a Fiji image processing application (Schindelin et al., 2012) and the trajectory of nuclear displacement was traced with a Particle Tracker plugin (Sbalzarini and Koumoutsakos, 2005) and a Manual Tracking plugin (Cordelières et al., 2013). The results of the tracking were graphed with a Chemotaxis and Migration Tool plugin (ibidi, Martinsried, Germany).

4.5. Immunostaining

Cryosections were reacted with monoclonal antibodies for NeuN (MAB377, Chemicon), HuC/D (16A11, Molecular Probes), followed by Alexa594-labeled anti-mouse IgG (Invitrogen). The GFP signal was enhanced using anti-GFP polyclonal antibody (A6455, Invitrogen) with an Alexa488-labeled secondary antibody (Invitrogen). Fluorescent images were captured with confocal laser scanning microscopy (FV300, Olympus).

Acknowledgments

The authors thank Drs Jun-ichi Miyazaki, Yoshiko Takahashi and Koichi Kawakami for providing pCAGGS vector, tol2-mediated transgene vectors.

Declarations of interest

None.Funding
This work was supported by JSPS KAKENHI Grant Number 15K06740 to Y.W.

References

Altman, J., Bayer, S.A., 1987a. Development of the precerebellar nuclei in the rat. II. The intramural olivary migratory stream and the neurogenetic organization of the inferior olive. J. Comp. Neurol. 257, 490–512.
Altman, J., Bayer, S.A., 1987b. Development of the precerebellar nuclei in the rat: III. The posterior precerebellar extramural migratory stream and the lateral reticular and external cuneate nuclei. J. Comp. Neurol. 257, 513–528.
Ambrosiani, J., Armengol, J.A., Martínez, S., Puelles, L., 1996. The avian inferior olive derives from the alar neuroepithelium of the rhombomeres 7 and 8: an analysis by using chick-quail chimeric embryos. Neuroreport 7, 1285–1288.
Anderson, S.A., Eisenstat, D.D., Shi, L., Rubenstein, J.L., 1997. Interneuron migration from basal forebrain to neocortex: dependence on Dlx genes. Science 278, 474–476.
Bielle, F., Griveau, A., Narboux-Neme, N., Vigneau, S., Sigrist, M., Arber, S., Wassef, M., Pierani, A., 2005. Multiple origins of Cajal-Retzius cells at the borders of the developing pallium. Nat. Neurosci. 8, 1002–1012.
Bourrat, F., Sotelo, C., 1988. Migratory pathways and neuritic differentiation of inferior olivary neurons in the rat embryo. Axonal tracing study using the in vitro slab technique. Brain Res. 467, 19–37.
Bourrat, F., Sotelo, C., 1990. Migratory pathways and selective aggregation of the lateral reticular neurons in the rat embryo: a horseradish peroxidase in vitro study, with special reference to migration patterns of the precerebellar nuclei. J. Comp. Neurol. 294, 1–13.
Butler, A.B., Hodos, W., 2005. Comparative Vertebrate Neuroanatomy: Evolution and Adaptation Second edition. Wiley interscience, 311–340, (Chapter 18).
Corbin, J.G., Nery, S., Fishell, G., 2001. Telencephalic cells take a tangent: non-radial migration in the mammalian forebrain. Nat. Neurosci. 4, 1177–1182.
Cordelières, F.P., Petit, V., Kumasaka, M., Debeir, O., Letort, V., Gallagher, S.J., Larue, L., 2013. Automated cell tracking and analysis in phase-contrast videos (iTrack4U): development of Java software based on combined mean-shift processes. PLoS One 8, e81266.
Cowan, W.M., Adamson, L., Powell, T.P.S., 1961. An experimental study of the avian visual system. J. Anat. 95, 545–563.
Domesick, V.B., Morest, D.K., 1977. Migration and differentiation of ganglion cells in the optic tectum of the chick embryo. Neuroscience 2, 459–475.
Funahashi, J.-I., Okafuji, T., Ohuchi, H., Noji, S., Tanaka, H., Nakamura, H., 1999. Role of Pax-5 in the regulation of a mid-hindbrain organizer's activity. Dev. Growth Differ. 41, 59–72.
Goldberg, S., 1974. Studies on the mechanics of devenopment of the visual pathways in the chick embryo. Dev. Biol. 36, 24–43.
Gray, G.E., Glover, J.C., Majors, J., Sanes, J.R., 1988. Radial arrangement of clonally related cells in the chicken optic tectum: lineage analysis with recombinant

retrovirus. Proc. Natl. Acad. Sci. USA 85, 7356–7360.
Gray, G.E., Sanes, J.R., 1991. Migratory paths and phenotypic choices of clonally related cells in the avian optic tectum. Neuron 6, 211–225.
Harkmark, W., 1954. Cell migration from the rhombic lip to the inferior olive, the nucleus raphe and the pons. A morphological and experimental investigation on chick embryos. J. Comp. Neurol. 100, 115–210.
Kawauchi, D., Taniguchi, H., Watanabe, H., Saito, T., Murakami, F., 2006. Direct visualization of nucleogenesis by precerebellar neurons: involvement of ventricle-directed, radial fibre-associated migration. Development 133, 1113–1123.
King, A.J., 2004. The superior colliculus. Curr. Biol. 14, R335–R338.
Lambert de Rouvroit, C., Goffinet, A.M., 2001. Neuronal migration. Mech. Dev. 105, 47–56.
LaVail, J.H., Cowan, W.M., 1971a. The development of the chick optic tectum. I. Normal morphology and cytoarchitectonic development. Brain Res. 28, 391–419.
LaVail, J.H., Cowan, W.M., 1971b. The development of the chick optic tectum. II. autoradiographic studies. Brain Res. 28, 421–441.
Marín, O., Rubenstein, J., 2001. A long, remarkable journey: tangential migration in the telencephalon. Nat. Rev. Neurosci. 2, 780–790.
Martínez, S., Puelles, L., Alvarado-Mallart, R.M., 1992. Tangential neuronal migration in the avian tectum: cell type identification and mapping of regional differences with quail/chick homotopic transplants. Dev. Brain Res. 66, 153–163.
Martini, F.J., Valiente, M., Bendito, G.L., Szabó, G., Moya, F., Valdeolmillos, M., Marín, O., 2009. Biased selection of leading process branches mediates chemotaxis during tangential neuronal migration. Development 136, 41–50.
McLoon, S.C., 1985. Evidence for shifting connections during development of the chick retinotectal projection. J. Neurosci. 5, 2570–2580.
Meyer, G., Perez-Garcia, C.G., Abraham, H., Caput, D., 2002. Expression of p73 and Reelin in the developing human cortex. J. Neurosci. 22, 4973–4986.
Nadarajah, B., Parnavelas, J.G., 2002. Modes of neuronal migration in the developing cerebral cortex. Nat. Rev. Neurosci. 3, 423–432.
Niwa, H., Yamamura, K., Miyazaki, J., 1991. Efficient selection for high-expression transfectants with a novel eukaryotic vector. Gene 108, 193–199.
Omi, M., Harada, H., Watanabe, Y., Funahashi, J.-I., Nakamura, H., 2014. Role of En2 in the tectal laminar formation of chick embryos. Development 141, 2131–2138.
Ono, K., Kawamura, K., 1989. Migration of immature neurons along tangentially oriented fibers in the subpial part of the fetal mouse medulla oblongata. Exp. Brain Res. 78, 290–300.
Parnavelas, J.G., 2000. The origin and migration of cortical neurones: new vistas. Trends Neurosci. 23, 126–131.
Placzek, M., Dale, K., 1999. Tissue recombinations in collagen gels. Methods Mol. Biol. 97, 293–304.
Puelles, L., Bendala, M.C., 1978. Differentiation of neuroblasts in the chick optic tectum up to eight days of incubation: a Golgi study. Neuroscience 3, 307–325.
Ramón y Cajal, S., 1911. Histologie du système nerveux de l'homme & des vertébrés. Vol. 2, Maloine, Paris.
Sato, Y., Kasai, T., Nakagawa, S., Tanabe, K., Watanabe, T., Kawakami, K., Takahashi, Y., 2007. Stable integration and conditional expression of electroporated transgenes in chicken embryos. Dev. Biol. 305, 616–624.
Sbalzarini, F., Koumoutsakos, P., 2005. Feature point tracking and trajectory analysis for video imaging in cell biology. J. Struct. Biol. 151, 182–195.
Schindelin, J., Arganda-Carreras, I., Frise, E., Kaynig, V., Longair, M., Pietzsch, T., Preibisch, S., Rueden, C., Saalfeld, S., Schmid, B., et al., 2012. Fiji: an open-source platform for biological-image analysis. Nat. Methods 9, 676–682.
Senut, M.C., Alvarado-Mallart, R.M., 1986. Development of the retinotectal system in normal quail embryos: cytoarchitectonic development and optic fiber innervation. Dev. Brian Res. 29, 123–140.
Sugiyama, S., Nakamura, H., 2003. The role of Grg4 in tectal laminar formation. Development 130, 451–462.
Takiguchi-Hayashi, K., Sekiguchi, M., Ashigaki, S., Takamatsu, M., Hasegawa, H., Suzuki-Migishima, R., Yokoyama, M., Nakanishi, S., Tanabe, Y., 2004. Generation of reelinpositive marginal zone cells from the caudomedial wall of telencephalic vesicles. J. Neurosci. 24, 2286–2295.
Tan, K., Le Douarin, N.M., 1991. Development of the nuclei and cell migration in the medulla oblongata. Application of the quail-chick chimera system. Anat. Embryol. 183, 321–343.
Villar-Cerviño, V., Molano-Mazón, M., Catchpole, T., Valdeolmillos, M., Henkemeyer, M., Martínez, L.M., Borrell, V., Marín, O., 2013. Contact repulsion controls the dispersion and final distribution of Cajal-Retzius cells. Neuron 77, 457–471.
Watanabe, Y., Nakamura, H., 2000. Control of chick tectum territory along dorsoventral axis by Sonic hedgehog. Development 127, 1131–1140.
Watanabe, Y., Sakuma, C., Yaginuma, H., 2014. NRP1-mediated Sema3A signals coordinate laminar formation in the developing chick optic tectum. Development 141, 3572–3582.
Watanabe, Y., Yaginuma, H., 2015. Tangential cell migration during layer formation of chick optic tectum. Dev. Growth Differ. 57, 539–543.